J.Natn.Sci.Foundation Sri Lanka 2015 43 (4): 347-355
DOI: http://dx.doi.org/10.4038/jnsfsr.v43i4.7969

RESEARCH ARTICLE

Coordinated inertia response from permanent magnet synchronous generator (PMSG) based wind farms

John Licari[1] and Janaka Ekanayake[2,3]*
[1]*Department of Industrial Electrical Power Conversion, Faculty of Engineering, University of Malta, Malta.*
[2]*Department of Electrical and Electronic Engineering, Faculty of Engineering, University of Peradeniya, Peradeniya.*
[3]*Institute of Energy, Cardiff University, UK.*

Revised: 13 July 2015; Accepted: 26 August 2015

Abstract: A simplified model of a wind turbine connected to the grid through a power electronic interface was developed to carry out inertia response studies. This model was validated using the detailed model simulation and experimental results. The results show that wind turbines provide inertia response for 3 − 4 s and then operate at reduced power until they return to their steady state operating point. As this could hinder the frequency recovery of the power system, the aggregated inertia response from a wind farm was investigated by delaying the frequency signal to the inertia controller of each turbine based on their status of operation. How local frequency measurements can be used for a wind farm connected through an AC network is also discussed. By connecting a number of wind turbine models in parallel and operating them under different wind speeds, frequency commands and inertia controller gains, it was demonstrated that an inertia response of more than 10 s can be provided by coordinating the inertia response of individual turbines.

Keywords: Frequency response, full rated power converter (FRPC) wind turbines, inertia response, wind turbine control.

INTRODUCTION

Many countries around the world are increasing their share of renewable energy generation. Renewable energy generation plants that are connected through power electronic converters such as wind and photovoltaic (PV) converters, do not provide the same natural frequency response as synchronous generators that release part of the kinetic energy stored in the rotating mass as frequency changes. Therefore adding renewable energy generation will result in a reduction of the overall inertia of the power system thus leading to unacceptable excursions of the grid frequency.

Although variable-speed wind turbines that are connected to the grid through a back-to-back power electronic converter do not provide natural inertia response, the converters can be controlled by using appropriate supplementary control action to force a wind turbine to contribute to system inertia. Several methods of achieving this emulated inertia response have been reported in literature (Lalor *et al*., 2005; Ramtharan *et al*., 2007; Conroy & Watson, 2008; Ekanayake *et al*., 2008; Ullah *et al*., 2008; Kayikci & Milanovic, 2009).

Recognizing the operating difficulties arising from a large penetration of wind, many power system operators are considering to make emulated inertia response from wind turbines mandatory. For example, the European draft code (ENTSO-E) requires an inertia response from a plant above an agreed size (ENTSO-E, 2012). Further, in the Hydro-Quebec grid codes an 'inertial response' from wind turbines is required to act during 'major frequency deviations' in order to help restore system frequency (Hydro-Quebec, 2009). To achieve this, wind power plants with a rated capacity greater than 10 MW should be equipped with a frequency control system that acts during frequency events. In the UK, the National Grid frequency response working group considered the inertia response capability of wind turbines and proposed a synthetic inertia response (NationalGrid, 2010). However, they decided not to include this requirement in the GB grid codes.

This paper demonstrates the possibility of offering emulated inertia response from wind turbines for below and above rated wind speeds using a detailed simulation model. The wind turbines considered are based on a permanent magnet synchronous generator (PMSG) with a fully rated power converter (FRPC). A simplified turbine model was developed and validated using the simulations from the detailed model and experimental results. Finally as an application, a number

*Corresponding author (EkanayakeJ@cardiff.ac.uk)

of parallel connected simplified turbine models were used to represent a cluster of wind turbines in a wind farm and their combined emulated inertia response was illustrated.

PERMANENT MAGNET SYNCHRONOUS GENERATOR (PMSG) WITH A FULLY RATED POWER CONVERTER (FRPC)

Figure 1 shows the components of a variable speed PMSG-FRPC wind turbine with its associated controllers. This was modelled in Simulink and all parameters of the wind turbine model are given in the Appendix.

The model consists of an aerodynamic model, a drive train, a PMSG, a fully rated back-to-back converter, a pitch controller and an inertia controller. The generator is coupled to the wind turbine rotor through a three-stage gearbox, which scales up the rotational speed of the rotor determined by the wind speed. The generator electrical side is connected to the grid through a power converter, which converts variable frequency power into DC and then inverts it to 50 Hz AC.

The aerodynamic model was described by

$$\tau_{aero} = \frac{0.5\pi\rho R^2 V_w^3 C_p(\lambda,\beta)}{\omega_{rot}} \quad ...(1)$$

where τ_{aero} is the aerodynamic torque (Nm), R is the blade radius (m), V_w is the wind speed (m/s), ρ is the air density (kg/m^3), ω_{rot} is the rotor speed (rad/s), C_p is the power coefficient, λ is the tip speed ratio and β is the pitch angle (Burton *et al*., 2001). The power coefficient C_p was taken from a look-up table derived from a generic 2 MW wind turbine model in Bladed.

A two-mass model was used to represent the mechanical dynamics. The equations used to describe the two-mass model are given by (Licari *et al*., 2012a),

$$J_{rot}\frac{d}{dt}\omega_{rot} = \tau_{aero} - K(\theta_1 - \theta_2) - D(\dot{\theta}_1 - \dot{\theta}_2) \quad ...(2)$$

$$J_{gen}\frac{d}{dt}\omega_{gen} = -\tau_{gen} - K(\theta_2 - \theta_1) - D(\dot{\theta}_2 - \dot{\theta}_1) \quad ...(3)$$

$$\frac{d}{dt}\theta_1 = \omega_{rot} \quad and \quad \frac{d}{dt}\theta_2 = \omega_{gen} \quad ...(4)$$

where τ_{aero} is the aerodynamic (Nm), τ_{gen} is the generator torque (Nm) referred to the low-speed shaft (LSS), ω_{rot} and ω_{gen} are the speeds of the rotor and generator (rad/s), θ_1 and θ_2 are the low and high speed shafts angular position (rad), J_{rot} and J_{gen} are the rotor and generator inertias (kgm^2), K and D are the stiffness coefficient (Nm/rad) and the damping coefficient (Nms/rad) referred to the LSS.

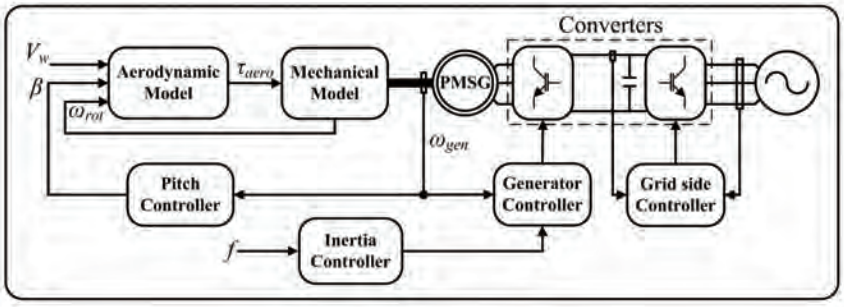

Figure 1: Block diagram of the PMSG-FRPC based wind turbine implemented in Simulink

The PMSG was modelled using the following well known equations (Krishnan, 2010):

$$v_{sd} = R_s i_{sd} + \frac{d}{dt}L_s i_{sd} - \omega_{gen} L_s i_{sq} \quad ...(5)$$

$$v_{sq} = R_s i_{sq} + \frac{d}{dt}L_s i_{sq} + \omega_{gen} L_s i_{sd} + \omega_{gen}\lambda_m \quad ...(6)$$

where L_s is the self-inductance of the stator (assuming no saliency) (H), v_{sd} and v_{sq} are equivalent stator voltages

$$\tau_{gen} = \frac{3}{2} p \lambda_m i_{sq} \quad ...(7)$$

in rotor (dq) frame (V), λ_m is the flux induced by the permanent magnets in stator (Vs), i_{sd} and i_{sq} are equivalent stator currents in the rotor (dq) frame (A) and p is the generator pole pairs.

The generator controller was derived assuming that the d-axis is aligned with the flux produced by the

permanent magnet, λ_m. The *q*-axis current was then used to control the electromagnetic torque of the generator. The reference torque τ^*_{opt} was set from an optimal torque look-up table for maximum power extraction. The *q*-axis current reference was obtained by passing the torque reference through a gain derived from equation (7). In the control scheme of the grid-side converter the *d*-axis current was used to control the DC-link voltage and thus the active power flow into the grid, whereas the *q*-axis current was used to control the reactive power flow.

For the above rated wind speeds, the aerodynamic torque was limited by a pitch angle controller. This controller consists of a PI controller equipped with an anti-windup circuit that generates a pitch angle reference from the generator speed error (Licari *et al*., 2012b). More details of the operation of generator and grid side converter controllers associated with PMSG-FRPC wind turbines can be found in Hansen and Michalke (2008) and Shuhui *et al*. (2012). The inertia controller shown in Figure 1 will be discussed in detail in the next section.

INERTIA RESPONSE FROM WIND TURBINES

Emulated inertia response: PMSG-FRPC based wind turbine

In order to obtain an emulated inertia response, a supplementary control signal created by two control loops is added to the generator-side torque controller as shown in Figures 1 and 2 (Ramtharan *et al*., 2007). The inputs to the controller is the frequency of the system *f* and the deviation *Δf*. One of the loops is related to the rate of change of frequency (*df/dt*) and the other to the deviation in the grid frequency (*Δf*). K_1 is a constant that determines the magnitude of the extra torque to be supplied to the generator (resulting into additional power output) during the frequency event. K_2 is another constant that is used to increase the time during which the wind turbine is providing the inertia response. This has a direct implication on the time where the wind turbine starts to recover the kinetic energy lost during the inertia response phase. This instant is characterised by the point at which the power supplied by the turbine is less than the steady state power supplied before the inertia response event.

To explain the operation of these control actions, it is assumed that initially only Loop 1 of Figure 2 is active and that the turbine is in steady-state ($\tau_{aero} = \tau^*_{gen}$) operating at a wind speed of 10 m/s shown as point A in Figure 3.

When there is a frequency drop, Loop 1 applies a torque (τ_{loop1}) proportional to the rate of change of frequency. This increases the generator torque demand, τ^*_{gen}, resulting in a new operation point B. At this point the aerodynamic torque τ_{aero} available is less than the demanded generator torque; hence, the rotor and the

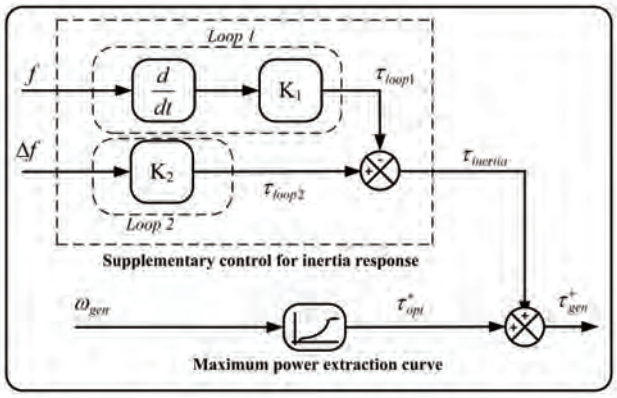

Figure 2: Inertia control loops [8]

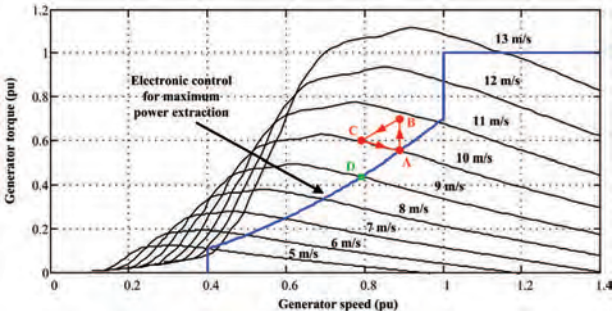

Figure 3: Torque *vs.* speed characteristics of a variable-speed wind turbine

generator start to slow down until a new operating point C is reached. This reduction in speed releases the kinetic energy of the rotating mass as inertia response. At this new rotational speed, the maximum power extraction curve output an optimal torque demand, τ^*_{opt}, for the generator controller (shown by point D). As the wind speed is unchanged (10 m/s), the aerodynamic torque τ_{aero}, is that corresponding to point C. The difference between the torque developed by the rotor and that demanded by τ^*_{opt} results in an accelerating torque, which moves the operation point from C back to A. During this process the generator operates at reduced power to re-establish the kinetic energy in the rotating mass. This effect is unwanted during inertia response because at the end of the inertia response (when the system frequency is stabilised), *df/dt* starts reducing to zero and as a consequence τ_{loop1} diminishes. This problem is mitigated by Loop 2. Apart from increasing the peak power during the inertia response, Loop 2 delays the start of the rotor acceleration period and thus the start of reduced power production (recovery phase).

The recovery phase is most significant during below rated wind speeds. This is because, at above rated wind speeds the excess wind power can be used to aid recovery. The inertia response for below and above rated wind speeds for different values of K_1 and K_2 is shown in Figure 4. It is worth noting that for above rated wind speeds the converters should have a transient power capability of 2 – 3 % above their continuous rating.

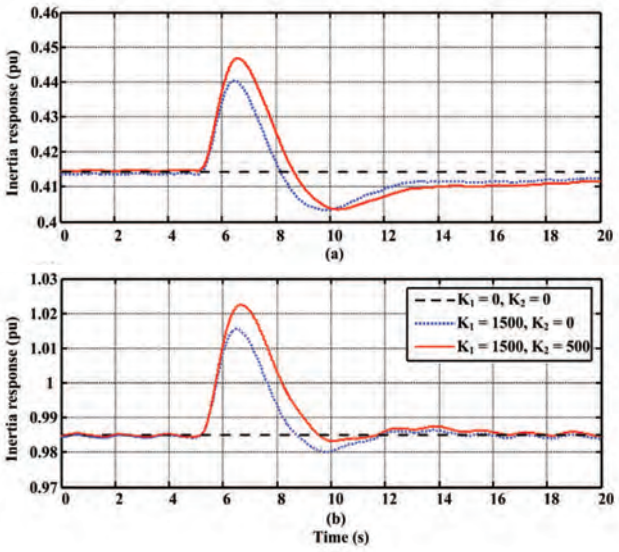

Figure 4: Inertia response (a) below rated wind speed (8.5 m/s) and (b) above rated wind speed (20 m/s)

SIMPLIFIED MODEL OF THE WIND TURBINE

As discussed previously, the inertia control loop modifies the torque set point of the generator controller. The generator controller then controls the generator stator current to have only a *q*-axis current component (*i.e.* $i_{sd} = 0$). Therefore equation (6) can be simplified to:

$$\frac{d}{dt}i_{sq} = -\frac{R_s}{L_s}i_{sq} + \frac{v_{sq} - \omega_{gen}\lambda_m}{L_s} \quad ...(8)$$

Rearranging equation (8) and multiplying L_s/R_s by yields,

$$\frac{L_s}{R_s}\frac{d}{dt}i_{sq} + i_{sq} = \frac{v_{sq} - \omega_{gen}\lambda_m}{R_s} \quad ...(9)$$

and in the Laplace domain, equation (9) is expressed as

$$\left(\frac{L_s}{R_s}s + 1\right)i_{sq} = \frac{v_{sq} - \omega_{gen}\lambda_m}{R_s} \quad ...(10)$$

The simplified model of FRPC-PMSG based wind turbine with the supplementary inertia control loop is shown in Figure 5. All the parameters and gains are given in the Appendix.

Laboratory prototype

An experimental platform with a rating of 1.3 kW was used to validate the inertia response provided by a single wind turbine. The platform can be divided into three sub systems: mechanical, electrical and control. The mechanical part consists of two AC brushless motors coupled by a flexible coupling where one was used as a motor and the other as a generator. An industrial speed drive was used to set the reference speed on the motor to emulate the speed of the high speed shaft of the generator. The output of the generator was connected to the grid through the electrical system composed of a back-to-back

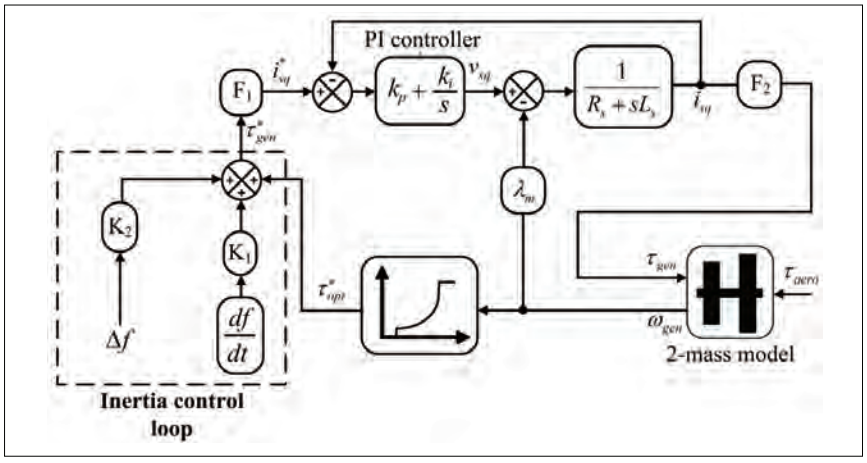

Figure 5: Block diagram of the simplified FRPC-PMSG based wind turbine with the inertia control loop

voltage source converter (VSC). The control system was divided into two levels: a low level controller and a high level controller. The main task of the low level controller was to control the power converters through vector control scheme. A sine-weighted PWM with a carrier frequency of 10 kHz was used for both VSCs. This controller was implemented on a TMS320F2808 digital signal processor. The high level controller was implemented on a dSPACE platform based on a DS1005 processor board and was used to model parts of the wind turbine such as the aerodynamics, pitch controller, inertia controller and the MPPT algorithm. Moreover, the high level controller provided the reference points for the motor speed and the low level controller.

The real-time experiment block diagram showing the hardware in-the-loop implementation is shown in Figure 6.

Simulation and experimental results

The detailed FRPC-PMSG wind turbine shown in Figure 1 and the simplified model shown in Figure 5

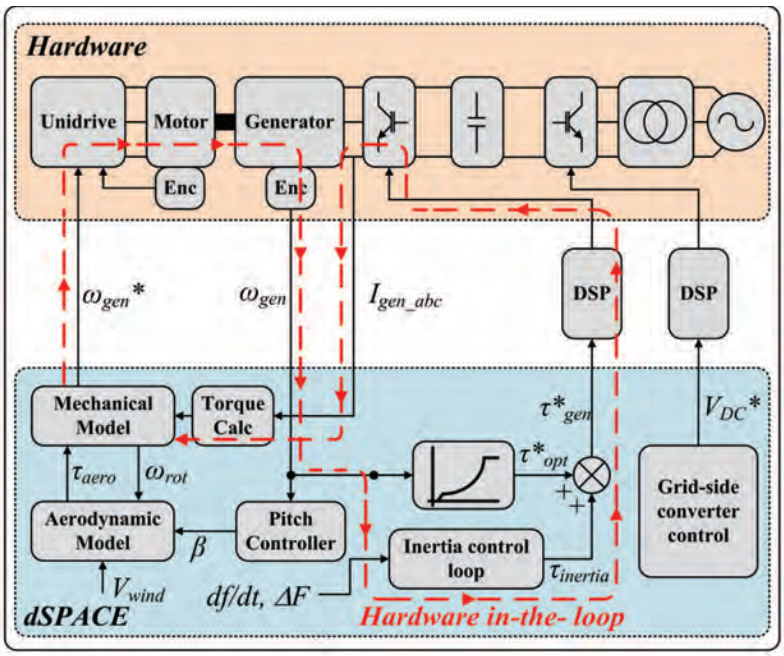

Figure 6: Experiment design block diagram showing the hardware in-the-loop

were both modelled in MATLAB/Simulink. In order to mimic a typical frequency change in a power system, the frequency variation shown in Figure 7 (a) was applied to the inertia control loop shown in Figure 5.

This inertia controller was added to the detailed model, simplified model and the laboratory rig. An inertia response of the FRPC-PMSG based wind turbine was obtained by changing the gains K_1 and K_2.

As the rating of the simulated system (2 MW) and laboratory model (1.3 kW) are quite different, the inertia response obtained was converted to p.u. on the respective machine bases (2 MW and 1.3 kW) and is shown in Figure 7 (b − d). Substantial agreement among the inertia responses can be seen. In the case of the simplified model simulation, the losses of the converters and other plants (assumed to be 0.5 %) were deducted from the power output of the generator.

An application study: inertia response from wind farm

In the previous section, inertia response from a single wind turbine was demonstrated. One of the main concerns of this response is the reduction in power after the inertia response has been shown. The typical system behaviour after a frequency event in the UK system is shown in Figure 8. The period between 0 to 10 s is the most critical for the power system as it needs support to arrest the collapsing frequency. Unfortunately after a short burst of power (3 − 4 s), the wind turbines output power will reduce in order to recover the

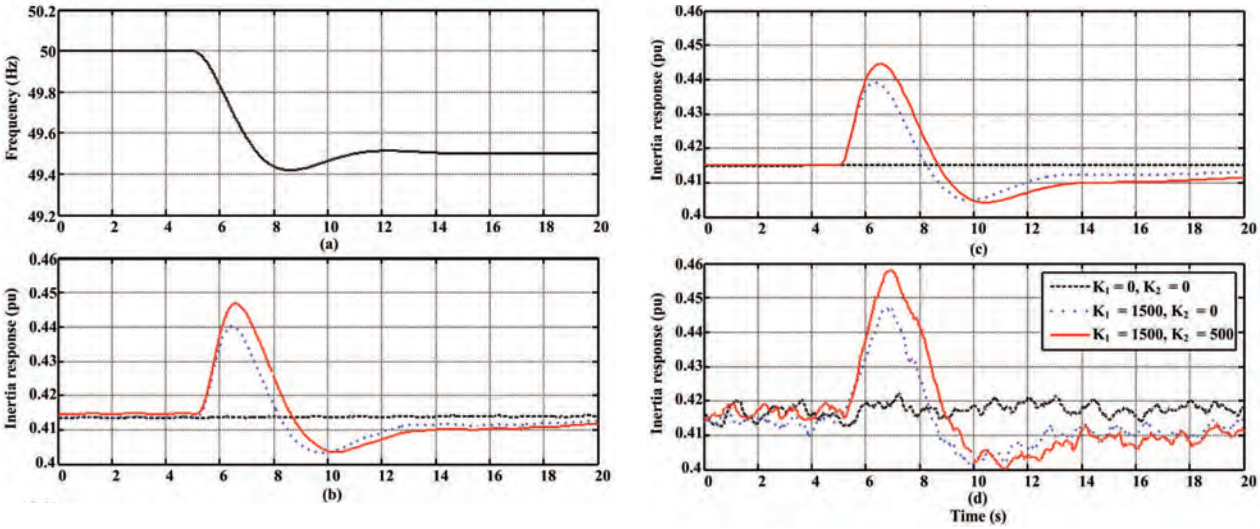

Figure 7: Inertia response (a) frequency deviation; (b) simulation- detailed model; (c) simulation - simplified model; (d) experiment (all values are with respect to the machine base)

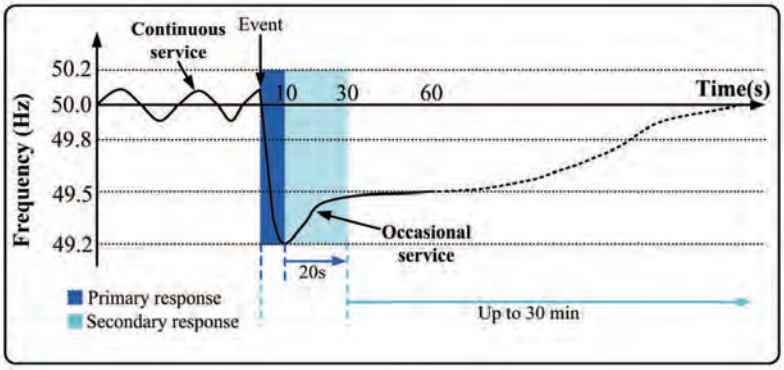

Figure 8: Frequency control in England and Wales (Erinmez *et al*., 1999)

kinetic energy extracted from the rotor. This under production of power will contribute further to increase the mismatch between generation and demand.

Although individual wind turbines provide rather poor inertia response performance, a wind farm could provide a better inertia response as it has a large number of generators and each operates individually. In order to demonstrate wind farm inertia response, a wind farm connected to the grid through AC networks (onshore wind farms and offshore wind farms with AC connections) is discussed.

The inertia controller of each wind turbine acts on a local frequency measurement but delays its response according to the status of the turbine (power output or speed, which directly correlates to the wind speed). Each inertia controller has a look-up table that determines the delay in bands, depending on the wind speed (or generator speed). Upon detecting a drop in frequency, the inertia controllers in the turbines that are operating at lower wind speeds act directly on the measured frequency signal. The turbines operating at a slightly higher wind speed will operate on the locally measured frequency signal delayed by a fraction of a second. Similarly the wind turbines operating on the next wind speed band will act on a further delayed frequency signal. The reason to schedule wind turbines this way can be explained using Figure 4. The wind turbines operating below the rated wind speed will have a large recovery power dip and that can be compensated by the inertia response from other wind turbines. As the recovery dip of the wind turbines operating above the rated wind speed is lower, scheduling them last will reduce the recovery dip of the entire wind farm.

In order to demonstrate a coordinated inertia response from a wind farm, each wind turbine in the wind farm shown in Figure 9 was modelled using the simplified model shown in Figure 5. In this demonstration, 10 clusters

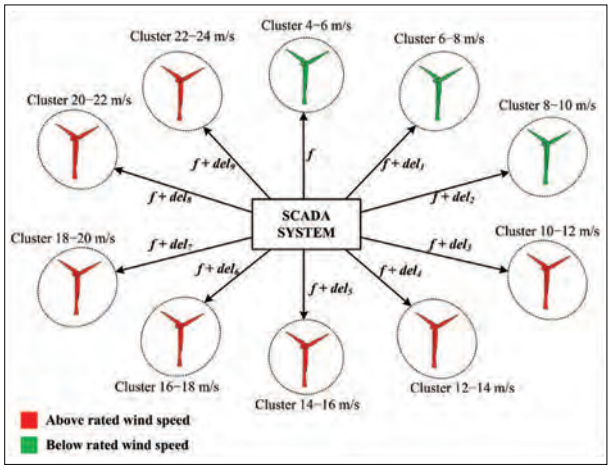

Figure 9: System considered for the wind farm inertia response

representing different wind speed bands (4 to 24 m/s) were used. The system was simulated in MATLAB/Simulink and the frequency signal shown in Figure 7 (a) (applied at 10 s) was used for the first cluster, and then it was delayed by different times ($del_{1\ to\ 9}$ in Figure 9) for the other clusters. It was assumed that the supervisory control and data acquisition (SCADA) has real-time information about the status of each wind turbine and the latency in the communication network is negligible.

Figure 10 shows the inertia response of the wind farm for frequency signals with different delays between clusters. It shows the response when each cluster had a fixed delay of 1 s or 1.5 s between two clusters and when the delay between the two clusters was variable with increasing intervals of 0.15 s (starting at 0.15 s between the first two clusters, 0.3 s between the next two clusters and so on) and

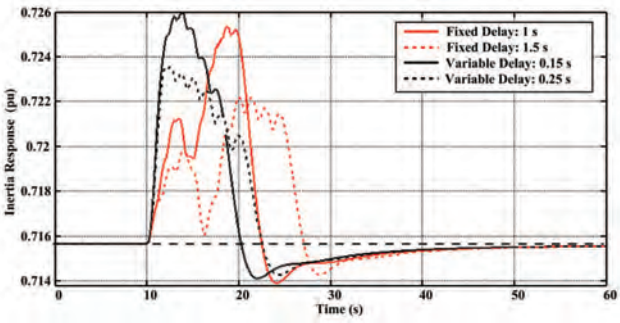

Figure 10: Inertia response from the wind farm

0.25 s (starting at 0.25 s between the first two clusters, then 0.5 s and so on). It can be clearly seen from the simulation results that the wind farm supports the grid during the critical period (0 −10 s) in all the different delay cases shown. However, the best performance was obtained with a variable delay of 0.15 s.

In order to demonstrate the flexibility and the improved performance that can be provided by a FRPC based wind farm, the response of the system shown in Figure 10 was compared to that of a similar system having fixed-speed induction generator (FSIG) wind turbines. In this simulation it was assumed that the inertia constant of each FSIG turbine is 6 s. In order to obtain the same peak inertia response from the FRPC based wind farm as in the case of the FSIG based wind farm, a variable

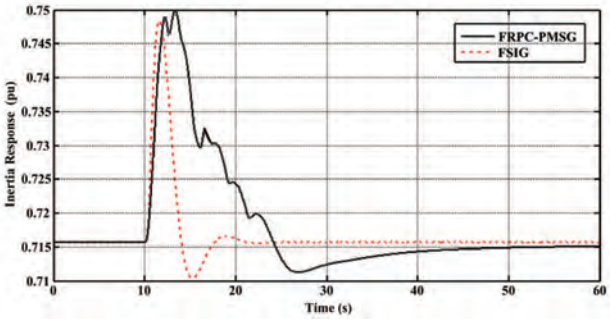

Figure 11: Comparison of inertia response from FSIG and FRPC based wind farms

delay between clusters of 0.15 s was used. Moreover, the values of K_1 and K_2 used were also variable; the cluster operating at the lowest wind speed band were set to a high level (K_1 = 6500 and K_2 = 3500), whereas those of the cluster operating at the highest wind speed band was set low (K_1 = 2000 and K_2 = 1250). Figure 11 shows the response obtained from a FSIG and FRPC-PMSG based wind farm.

CONCLUSION

The possibility of extracting inertia response from a single wind turbine and a wind farm that employs a PMSG with back-to-back power electronic converters was shown. It was demonstrated that the peak inertia response and the duration can be varied by changing the delay introduced to the frequency signal and gains of the inertia control loop of each wind turbine. By grading both the frequency signal delays and the inertia loop gains, the peak emulated response provided by the FRPC-PMSG based wind farm was made comparable to a FSIG based wind farm. Moreover, the starting time of the recovery period was delayed from about 4 s (FSIG) to about 15 s

(FRPC-PMSG). Since in the FRPC based wind farm the recovery starts after 10 s, it means that collectively each turbine supports the frequency recovery of the power system.

REFERENCES

1. Burton T., Sharpe D., Jenkins N. & Bossanyi E.A. (2001). *Wind Energy Handbook,* 2nd edition. John Wiley & Sons Ltd., New Jersey, USA.
   DOI: http://dx.doi.org/10.1002/0470846062
2. Conroy J.F. & Watson R. (2008). Frequency response capability of full converter wind turbine generators in comparison to conventional generation. *IEEE Transactions on Power Systems* **23**: 649 − 656.
   DOI: http://dx.doi.org/10.1109/TPWRS.2008.920197
3. Ekanayake J., Jenkins N. & Strbac G. (2008). Frequency response from wind turbines. *Wind Engineering* **32**: 573 − 586.
   DOI: http://dx.doi.org/10.1260/030952408787548811
4. ENTSO-E (2012). ENTSO-E Draft Network Code for Requirements for Grid Connection applicable to all Generators. Available at *https://www.entsoe.eu/fileadmin/user_upload/_library/consultations/Network_Code_RfG/120124_Network_Code_for_Requirements_forGrid_Connection_applicable_to_all_Generators.pdf#search=Grid%20Connection%20Applicable%20to%20all%20Generators,* Accessed 24 October 2014.
5. Erinmez I.A., Bickers D.O., Wood G.F. & Hung W.W. (1999). NGC experience with frequency control in England and Wales-provision of frequency response by generators. *Power Engineering Society 1999 Winter Meeting, IEEE,* volume 1, pp. 590 – 596.
   DOI: http://dx.doi.org/10.1109/PESW.1999.747521
6. Hansen A.D. & Michalke G. (2008). Modelling and control of variable-speed multi-pole permanent magnet synchronous generator wind turbine. *Wind Energy* **11**: 537 − 554.
   DOI: http://dx.doi.org/10.1002/we.278
7. Hydro-Quebec Trans Energie (2009). Transmission provider technical requirements for the connection of power plants to the Hydro-Quebec transmission system. Available at *http://www.hydroquebec.com/transenergie/fr/commerce/pdf/exigence_raccordement_fev_09_en.pdf,* Accessed June 2013
8. Kayikci M. & Milanovic J.V. (2009). Dynamic contribution of DFIG-based wind plants to system frequency disturbances. *IEEE Transactions on Power Systems* **24**: 859 − 867.
9. Krishnan R. (2010). *Permanent Magnet Synchronous and Brushless DC Motor Drives,* 1st edition. Taylor and Francis Group, New York, USA.
10. Lalor G., Mullane A. & O'Malley M. (2005). Frequency control and wind turbine technologies. *IEEE Transactions on Power Systems* **20**: 1905 − 1913.
    DOI: http://dx.doi.org/10.1109/TPWRS.2005.857393
11. Licari J., Ugalde-Loo C.E., Liang J., Ekanayake J. & Jenkins N. (2012a). Torsional damping considering both shaft and blade flexibilities. *Wind Engineering* **36**: 181 – 196.
    DOI: http://dx.doi.org/10.1260/0309-524X.36.2.181
12. Licari J., Ugalde-Loo C.E., Ekanayake J. & Jenkins N. (2012b). Comparison of the performance of two torsional vibration dampers considering model uncertainties and parameter variation. *European Wind Energy Association (EWEA) Annual Event 2012,* 16 – 19 April, Copenhagen, Denmark.
13. NationalGrid (2010). NGC frequency response technical sub-group. Available at *http://www.nationalgrid.com/NR/rdonlyres/F0793C0C-9617-49B1-98D4-FAC711F344ED/44455/Meeting2Presentation.pdf,* Accessed August 2013
14. Ramtharan G., Ekanayake J.B. & Jenkins N. (2007). Frequency support from doubly fed induction generator wind turbines. *Renewable Power Generation, IET* **1**: 3 − 9.
    DOI: http://dx.doi.org/10.1049/iet-rpg:20060019
15. Shuhui L., Haskew T.A., Swatloski R.P. & Gathings W. (2012). Optimal and direct-current vector control of direct-driven PMSG wind turbines. *IEEE Transactions on Power Electronics* **27**: 2325 − 2337.
    DOI: http://dx.doi.org/10.1109/TPEL.2011.2174254
16. Ullah N.R., Thiringer T. & Karlsson D. (2008). Temporary primary frequency control support by variable speed wind turbines; potential and applications. *IEEE Transactions on Power Systems* **23**: 601 − 612.
    DOI: http://dx.doi.org/10.1109/TPWRS.2008.920076

Appendix

Wind turbine parameters

Wind turbine: Power rating = 2 MW, Rotor radius = 40 m, Rated speed = 18 rpm, Blades = 3.

Mechanical model referred to LSS: J_{rot}= 6.0289×10^6 kgm^2, J_{gen}= 416633 kgm^2, K=1.6×10^8 Nm/rad, D = 250×10^3 Nms/rad, *Gearbox ratio* =83.33:1.

Generator: Poles = 4, Frequency = 50 Hz, Stator resistance R_s = 4.523 mΩ, L_s = 322 μH, λ_m = 1.75 Vs.

VSC: DC link capacitor (C): 90,000 μF, DC link voltage: 1400 V.

*Grid:*Grid Line-Line rms voltage (V_{LL}): 690 V, Grid coupling inductance (L_{grid}): 500 μH, Grid coupling resistance (R_{grid}): 0.4 mΩ

Control parameters

Generator PI:(current loop−kP = 0.166, k_I = 33.95); *Grid PI*: *(current loop −kP* = 0.122, k_I = 39.3, *voltage loop* − k_P = 9.6, k_I = 240); *Pitch controller:* ($k_P = 4.93\times10^{-3}$, $k_I = 1.7\times10^{-3}$)

Other parameters

Air density (ρ): 1.225 kg/m^3, Cut-in wind speed: 4 m/s, Cut-out wind speed: 24 m/s, Rated wind speed: 12 m/s

Simplified model gains

$$F_1 = \frac{2}{3}\frac{1}{p\lambda_m};\ F_2 = \frac{3}{2}p\lambda_m$$